Dalton Transactions

PAPER

View Article Online
View Journal | View Issue

Cite this: *Dalton Trans.*, 2017, **46**, 9415

Enhancement of the lithium ion conductivity of Ta-doped $Li_7La_3Zr_2O_{12}$ by incorporation of calcium†

Hany El-Shinawi,[a] Edmund J. Cussen *[b] and Serena A. Corr *[a]

Received 29th April 2017,
Accepted 25th June 2017

DOI: 10.1039/c7dt01573a

rsc.li/dalton

Fast ion conducting garnet materials have been identified as promising electrolytes for all solid-state batteries. However, reliable synthetic routes to materials with fully elucidated cation site occupancies where an enhancement in lithium conductivity is observed remains a challenge. Ca-Incorporation is developed here as a promising approach to enhance the ionic conductivity of garnet-type $Li_{7-x}La_3Zr_{2-x}Ta_xO_{12}$ phases. Here we present a new sol–gel synthetic strategy as a facile route to the preparation of materials of a desired stoichiometry optimized for Li^+ conductivity. We have found that the ionic conductivity of $Li_{6.4}La_3Zr_{1.4}Ta_{0.6}O_{12}$ is increased by a factor of four by the addition of 0.2 mol of Ca per formula unit. Ca is incorporated in the garnet lattice where it has no effect on the sinterability of the material and is predominately located at the La sites. We anticipate that the ease of our synthetic route and the phases presented here represents a starting point for the further realization of solid state electrolyte compositions with similarly high Li^+ conductivities using this methodology.

Introduction

Fast-ion conducting $Li_7La_3Zr_2O_{12}$-derived garnets are potential ceramic components for Li^+ solid electrolyte membranes, a key component in next-generation all-solid-state and hybrid lithium batteries. $Li_7La_3Zr_2O_{12}$ is stable in contact with lithium metal and in aqueous solution,[1,2] exhibiting fast-ion conducting properties ($\sigma > 1 \times 10^{-4}$ S cm^{-1}) when sintered at elevated temperatures in an alumina crucible due to Al^{3+} incorporation.[1,3] The Al^{3+} dopant ions reside at the Li^+ sites thereby creating vacancies and stabilizing the fast-ion conducting cubic phase.[4,5] The unreliability of this synthesis due to uncontrollable reactions with the crucible, in conjunction with possible blocking of the Li^+ pathways by the Al^{3+} dopant ions,[6] has directed interest toward aliovalent doping at the Zr site in order to create equivalent Li^+ vacancies. Ta-Doped phases ($Li_{7-x}La_3Zr_{2-x}Ta_xO_{12}$) have attracted particular interest because the parent $Li_5La_3Ta_2O_{12}$ garnet displays excellent stability in contact with lithium metal.[7] Similar to $Li_5La_3Ta_2O_{12}$, Ta-rich $Li_{7-x}La_3Zr_{2-x}Ta_xO_{12}$ phases are difficult to sinter and possess relatively low Li^+ conductivity.[8] On the other hand, Zr-rich phases, similar to $Li_7La_3Zr_2O_{12}$, have shown an undesirable tendency to react with the alumina crucibles at elevated temperatures which greatly affects the reliability and reproducibility of the synthesis process.[8–11] Zr-Rich phases such as $Li_{7-x}La_3Zr_{2-x}Ta_xO_{12}$ (where x ranges from 0.25 to 0.6) have shown total conductivities ranging between 2×10^{-6} and 9×10^{-4} S cm^{-1} depending on whether the sintering process is performed in the absence or the presence of alumina, respectively.[8–11] The ionic conductivity is also strongly dependent on the densification procedure (*e.g.* hot-pressing)[12–15] and sintering temperature and time. Al^{3+} incorporation in this system, however, has not been fully characterized yet and the role of Al as a dopant and/or as a sintering aid is still ambiguous. Alternative approaches to densifying and enhancing the ionic conductivity of these materials are therefore required. In this study, we have developed a new sol–gel approach to synthesize these important phases and consider for the first time the improvement of the Li^+ conductivity by Ca-incorporation. The materials are synthesized at calcination temperatures as low as 900 °C and demonstrate a significant improvement of the Li^+ conductivity by Ca-incorporation of up to 0.2 mole. The synthesis and characterization of pure $Li_{6.4}La_3Zr_{1.4}Ta_{0.6}O_{12}$ and the Ca-doped derivative are presented here.

Results and discussion

The materials are prepared using the sol–gel procedure described in Fig. 1 (see ESI† for experimental details).

[a]*School of Chemistry, WestCHEM, University of Glasgow, Glasgow G12 8QQ, UK. E-mail: serena.corr@glasgow.ac.uk*
[b]*WestCHEM, Department of Pure and Applied Chemistry, The University of Strathclyde, Thomas Graham Building, 295 Cathedral Street, Glasgow, G1 1XL, UK. E-mail: edmund.cussen@strath.ac.uk*

†Electronic supplementary information (ESI) available. See DOI: 10.1039/c7dt01573a

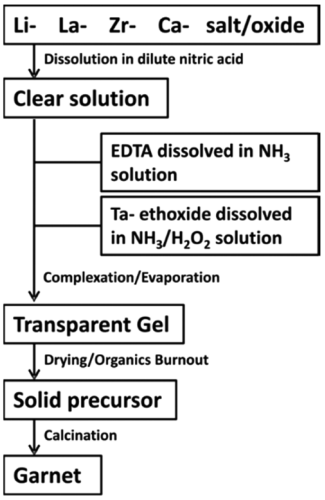

Fig. 1 A schematic representation of the sol–gel procedure used to synthesize pure and Ca-containing $Li_{6.4}La_3Zr_{1.4}Ta_{0.6}O_{12}$.

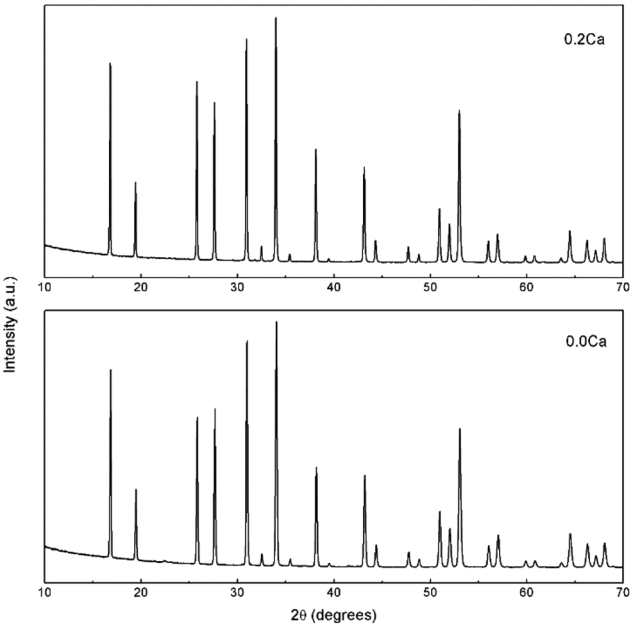

Fig. 2 XRD patterns of pure and Ca-containing $Li_{6.4}La_3Zr_{1.4}Ta_{0.6}O_{12}$ calcined at 900 °C.

$Li_{7-x}La_3Zr_{2-x}Ta_xO_{12}$ phases are typically prepared *via* solid-state reactions employing several homogenization (*e.g.* ball milling) and calcination steps at temperatures up to 1140 °C.[8–11] The previously reported solution-based syntheses either employ a coprecipitation procedure in which Ta-containing alcohol solutions and Li/La/Zr-containing aqueous solutions are mixed,[12–14] or, in one report,[16] the use of a sol–gel procedure followed by ball milling steps and high temperature calcination in order to obtain sufficiently pure phases. In our synthesis, Ta^{5+} is instead stabilized in aqueous ammonia solution by the addition of excess H_2O_2, whereupon an ammonium tantalum-peroxo-complex is formed.[17,18] This procedure, which is highly reproducible, ensures there is a homogeneous mixing of the reactants. Therefore, a 2 h calcination of the solid precursor at 900 °C was sufficient to produce high purity phases and there is no requirement for prolonged heating at elevated temperatures or any ball-milling.

Fig. 2 shows the X-ray diffraction (XRD) patterns of pure and Ca-containing (0.2 mole pfu) $Li_{6.4}La_3Zr_{1.4}Ta_{0.6}O_{12}$. The patterns indicate that the synthesized materials are predominantly single-phase. Induced coupled plasma-mass spectroscopy (ICP-MS) indicates that the La : Ca molar ratio in the Ca-doped material is 2.9 : 0.185(1), which is in agreement with the reaction stoichiometry (2.9 : 0.2) and the results of energy-dispersive X-ray spectroscopy (EDX) analysis. EDX elemental maps reveal a homogeneous distribution of Ca in the material (Fig. S1†), which suggests that Ca is incorporated in the garnet phase.

In an attempt to locate Ca in the garnet structure, neutron diffraction data were collected from the material at room temperature and the structure was refined simultaneously against X-ray and neutron diffraction data. Neutron diffraction data were collected using the Polaris instrument at Rutherford Appleton Laboratories (UK), and a Rietveld structure refinement was performed using the GSAS suite of programs. The refinement revealed the absence of any Ca-containing secondary phases. A small amount of lithium carbonate was detected as a secondary phase, and was introduced in the structure refinement. The presence of this impurity is consistent with the use of an excess of lithium in the synthesis process, and the exposure of the material to atmospheric air.[19] The structure refinement was performed with the garnet framework atoms La, Zr/Ta, and O located at the 24c sites, 16a sites, and 96h sites, respectively. Lithium is allowed to distribute over the tetrahedrally coordinated 24d sites, and the 48g and 96h sites that both exist inside heavily distorted oxide octhedra.[10] The refinement was initiated by allowing Ca^{2+} to replace La^{3+} at the 24c sites as anticipated from ionic radii considerations.[20,21] By introducing vacancies at the 24c sites, refining the Ca content in these sites, and allowing Li occupancies across the 24c, 16a, and 96h sites to refine freely, our refinement revealed the incorporation of 0.22(2) mole Ca pfu in the material, which agrees with the value suggested by ICP-MS analysis (~0.19 mole pfu). Based on the results of this refinement we assign a composition of $Li_{6.3}La_{2.9}Ca_{0.2}Zr_{1.4}Ta_{0.6}O_{12}$ to this garnet phase, in good agreement with the stoichiometry of the reagents. The fitted NPD and XRD patterns are shown in Fig. 3 and Fig. S2,† respectively, and the structural parameters used in the refinement are summarized in Table S1.†

Previous studies of $Li_{5+x}La_{3-x}Ca_xTa_2O_{12}$ have consistently located Ca at the La 8-coordinate sites.[20–23] However, the introduction of Ca^{2+} to replace Zr^{4+} at the 16a octahedral sites has recently been suggested by neutron diffraction studies in $Li_7La_3Zr_2O_{12}$.[25] Due to the complex disordered arrangement of multiple cations and vacancies it is not possible to unambiguously rule this out even using complementary information provided by a combined analysis of X-ray and neutron data. Considering the bond valence sums for Ca^{2+} on these two sites

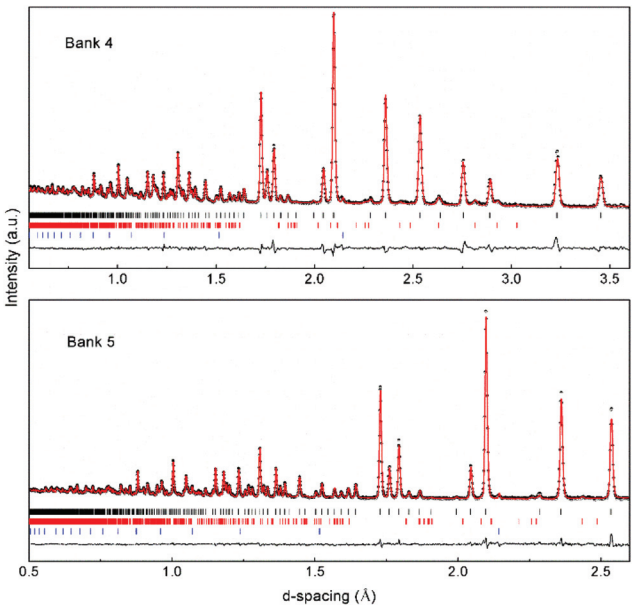

Fig. 3 Rietveld fits to Polaris neutron diffraction data for $Li_{6.3}La_{2.9}Ca_{0.2}Zr_{1.4}Ta_{0.6}O_{12}$ calcined at 900 °C. The top markers (black) are for the garnet phase; the middle markers (red) are for Li_2CO_3; the bottom markers (blue) are for V (from the vanadium can used in the measurement).

shows that the larger site, with a calculated valence for calcium of +1.66, is undoubtedly a much better match to the bonding requirements of Ca than the much smaller octahedral Zr site, with an unacceptably high bond valence sum for calcium of +4.43.

The Li^+ transport properties of pure $Li_{6.4}La_3Zr_{1.4}Ta_{0.6}O_{12}$ and $Li_{6.3}La_{2.9}Ca_{0.2}Zr_{1.4}Ta_{0.6}O_{12}$ were studied by impedance spectroscopy in order to investigate the influence of Ca-incorporation on the Li^+ conductivity. Impedance spectra were recorded from cold- and hot-pressed samples (at 1000 °C) in the temperature range of 25 to 130 °C using gold blocking electrodes. Fig. S3† shows the scanning electron microscopy (SEM) images of the surface of different pellets used in the impedance study. Pellets formed by cold pressing clearly show poorer sintering behavior compared with hot-pressed pellets. The hot-pressed pure and Ca-doped samples showed relative densities of ~88% and ~89% respectively, indicating approximately similar sinterability. This excludes the effect of sinterability on the relative ionic conductivities of the two materials and allows the study of the influence of Ca-inclusion on the ionic conductivity in this system. It should be noted that optimizing the hot pressing procedure to obtain higher relative densities, and consequently higher ionic conductivities, is not considered in this study. XRD patterns of the hot-pressed samples indicate that the samples retain the garnet structure with high crystallinity (Fig. S4†). Fig. S4† shows the emergence of a small impurity peak in the diffraction pattern, which we have assigned as $Li_4Zr_3O_8$ and arises as a result of the heating process. There is a negligible amount of this phase present and therefore will not affect the subsequent impedance analysis.

Fig. 4 displays typical Nyquist impedance plots of different samples at room temperature. In Fig. 4a, the plots collected from the cold-pressed samples are formed of two unresolved semicircles and a linear low-frequency tail. The two semicircles become clearly resolvable after hot pressing (Fig. 4b). The impedance data were successfully fitted using conventional equivalent circuits that employ a constant phase element in parallel to a resistance element to represent a semicircle ([RQ]), and a constant phase element to represent the low frequency response ([Q]) (Fig. 4). In hot-pressed samples, the high-frequency and the intermediate-frequency semicircles clearly correspond to bulk and grain-boundary resistances, respectively. The observation of the low-frequency tails in all samples is associated with the use of gold blocking electrodes and suggests that the transport effect is mainly ionic. The plots in Fig. 4 suggest that the total conductivity of $Li_{6.4}La_3Zr_{1.4}Ta_{0.6}O_{12}$ is improved by a factor of approximately four by calcium incorporation. The hot-pressed samples show

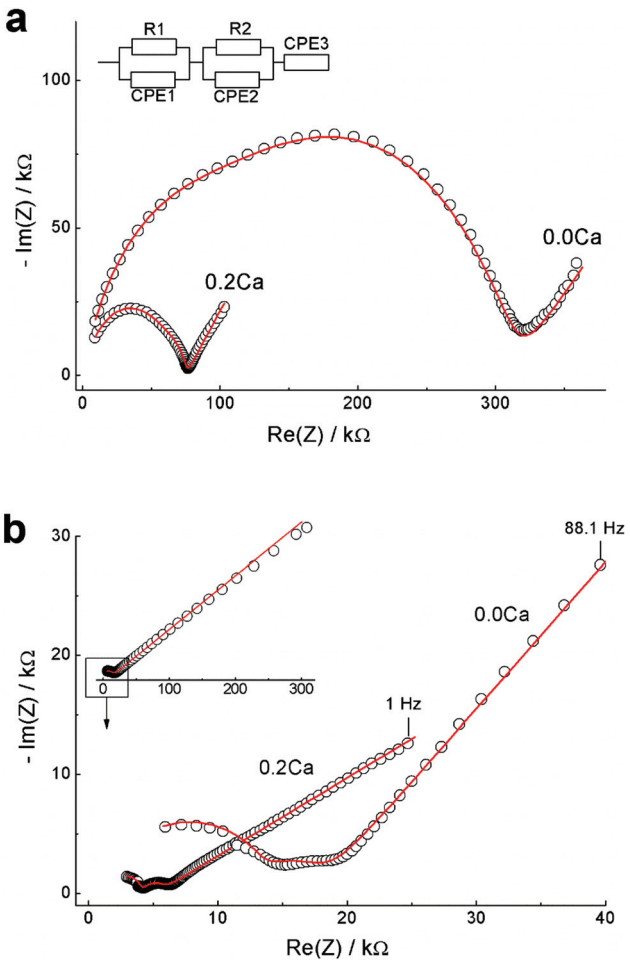

Fig. 4 (a) Typical impedance plots of cold-pressed pure $Li_{6.4}La_3Zr_{1.4}Ta_{0.6}O_{12}$ and $Li_{6.3}La_{2.9}Ca_{0.2}Zr_{1.4}Ta_{0.6}O_{12}$ using gold electrodes at room temperature; data were fitted using the presented equivalent circuit [RQ][RQ][Q]. (b) Typical impedance plots of hot-pressed pure $Li_{6.4}La_3Zr_{1.4}Ta_{0.6}O_{12}$ and $Li_{6.3}La_{2.9}Ca_{0.2}Zr_{1.4}Ta_{0.6}O_{12}$ at room temperature.

total conductivities of 5×10^{-5} S cm^{-1} and 2.0×10^{-4} S cm^{-1}, for pure $Li_{6.4}La_3Zr_{1.4}Ta_{0.6}O_{12}$ and $Li_{6.3}La_{2.9}Ca_{0.2}Zr_{1.4}Ta_{0.6}O_{12}$ respectively. The former value is consistent with those reported for Al-free $Li_{7-x}La_3Zr_{2-x}Ta_xO_{12}$ phases of similar composition.[8] Sakamoto *et al.*, however, have reported higher conductivity values for pure $Li_{6.5}La_3Zr_{1.5}Ta_{0.5}O_{12}$,[14] but the samples in this case were hot-pressed at 1050 °C and had relative densities greater than 97%. The Ca-doped material displays comparable transport properties to the previously reported Al-containing phases having similar composition and sinterability.[9,11,15,16] The Al-containing phases, however, are prepared through multistep, unreliable reactions with the alumina crucible at temperatures of up to 1140 °C. Calcium containing garnets have been reported at lower sintering temperatures of 790 °C, through the use of Al_2O_3 and Li_3BO_3 additives.[24] The Ca-doped material presented here, on the other hand, is synthesized at a relatively low calcination temperature (900–1000 °C) through a 2–3 h calcination step without the need for additives, which enhances the reliability of the synthesis process.

Impedance spectra of pure $Li_{6.4}La_3Zr_{1.4}Ta_{0.6}O_{12}$ and $Li_{6.3}La_{2.9}Ca_{0.2}Zr_{1.4}Ta_{0.6}O_{12}$ were recorded in the temperature range 25 °C to 130 °C in order to determine the activation energy for the Li^+ transport in these garnets (Fig. S5 and S6†). Studies of the hot-pressed samples revealed Li^+ conduction activation energies of 0.43(2) and 0.36(1) eV for the pure and Ca-containing samples, respectively. The Ca-doped sample hence exhibits enhanced Li^+ transport properties compared with the undoped material, which demonstrates the potential of Ca-doping as a promising approach to enhance the transport properties of $Li_{7-x}La_3Zr_{2-x}Ta_xO_{12}$ mixed garnets. It has been suggested that the incorporation of large alkaline earth cations, *e.g.* Ba^{2+}, into the La sites in $Li_5La_3Ta_2O_{12}$ will provide broader Li^+ conduction pathways leading to an improved Li^+ mobility in $Li_6ALa_2Ta_2O_{12}$ (A = Sr or Ba).[20,21] This clearly does not apply to Ca since Ca^{2+} with a radius of 1.12 Å is slightly smaller than La^{3+} at 1.16 Å. Here, in the case of Zr-rich $Li_{7-x}La_3Zr_{2-x}Ta_xO_{12}$ phases, we observe a significant improvement of Li^+ transport properties by incorporation of a small amount of Ca. Our observation is consistent with studies[25] which demonstrate enhanced transport properties in $Li_7La_3Zr_2O_{12}$ due to the incorporation of a small amount of Ca (0.05 occupancy) which was assigned to occupy the Zr sites. In our structural study of $Li_{6.3}La_{2.9}Ca_{0.2}Zr_{1.4}Ta_{0.6}O_{12}$, bond valence sums indicate that occupancy of the Zr site by Ca^{2+} is highly unfavorable with a calculated bond valence of +4.43. The unsuitability of this site for Ca^{2+} can be illustrated by comparing the ionic radii for these two cations in octahedral coordination; r_{Zr} is 0.72 Å whilst r_{Ca} is 1.00 Å.[26] Any incorporation of Ca^{2+} into these octahedra will introduce enormous compressive strain on the metal oxide bonds.

Conclusions

Ca-Incorporation is therefore demonstrated to be a promising approach to enhance the ionic conductivity of the functional Zr-rich $Li_{7-x}La_3Zr_{2-x}Ta_xO_{12}$ phases. By using a new, tailored sol–gel synthesis, it is possible to prepare fast Li-conducting garnets at significantly milder reaction conditions and so avoid the reproducibility problems often associated with previously reported syntheses. Our study on $Li_{6.3}La_{2.9}Ca_{0.2}Zr_{1.4}Ta_{0.6}O_{12}$suggests that Ca^{2+} is incorporated in the garnet lattice and resides at the La sites. The inclusion of Ca improves the Li^+ conductivity of $Li_{6.4}La_3Zr_{1.4}Ta_{0.6}O_{12}$ by a factor of approximately four. Ca does not act as a sintering aid and hence the improvement of the Li^+ conductivity is directly related to Ca incorporation in the garnet lattice. The Ca-doped material shows a bulk conductivity of 3.5×10^{-4} S cm^{-1} and a Li^+ conduction activation energy of 0.36(1) eV, suggesting a facile Li^+ diffusion in the material associated with Ca-inclusion.

Acknowledgements

This work was supported by funding from the EPSRC (EP/N001982/1) and we thank the School of Chemistry at the University of Glasgow for support. The authors gratefully acknowledge the allocation of beamtime at the Polaris beamline at the ISIS Neutron and Muon Source and the help of Dr Ron Smith with measurements. We are also grateful to Mr Michael Beglan and Mr Peter Chung for technical support. We also acknowledge Dr Srinivas Popuri and Dr Jan-Willem Bos for help with hot-pressing of pellets.

The data underpinning this paper are stored in the Enlighten: Research Data repository at the University of Glasgow: DOI: 10.5525/gla.researchdata.435.

References

1 R. Murugan, V. Thangadurai and W. Weppner, *Angew. Chem., Int. Ed.*, 2007, **46**, 7778.
2 C. Ma, E. Rangasamy, C. Liang, J. Sakamoto, K. L. More and M. Chi, *Angew. Chem., Int. Ed.*, 2015, **54**, 129.
3 C. A. Geiger, E. Alekseev, B. Lazic, M. Fisch, T. Armbruster, R. Langner, M. Fechtelkord, N. Kim, T. Pettke and W. Weppner, *Inorg. Chem.*, 2011, **50**, 1089.
4 H. Buschmann, J. Doelle, S. Berendts, A. Kuhn, P. Bottke, M. Wilkening, P. Heitjans, A. Senyshyn, H. E. Ehrenberg, A. Lotnyk, V. Duppel, L. Kienle and J. Janek, *Phys. Chem. Chem. Phys.*, 2011, **13**, 19378.
5 A. A. Hubaud, D. J. Schroeder, B. Key, B. J. Ingram, F. Dogan and J. T. Vaughey, *J. Mater. Chem. A*, 2013, **1**, 8813.
6 D. O. Shin, K. Oh, K. M. Kim, K.-Y. Park, B. Lee, Y.-G. Lee and K. Kang, *Sci. Rep.*, 2015, **5**, 18053.
7 V. Thangadurai, H. Kaack and W. J. F. Weppner, *J. Am. Ceram. Soc.*, 2003, **86**, 437.
8 H. Buschmann, S. Berendts, B. Mogwitz and J. Janek, *J. Power Sources*, 2012, **206**, 236.
9 Y. Wang and W. Lai, *Electrochem. Solid-State Lett.*, 2012, **15**, A68.

10 Y. Li, J. T. Han, C. A. Wang, H. Xie and J. B. Goodenough, *J. Mater. Chem.*, 2012, **22**, 15357.
11 K. Liu, J. T. Ma and C. A. Wang, *J. Power Sources*, 2014, **260**, 109.
12 J. L. Allen, J. Wolfenstine, E. Rangasamy and J. Sakamoto, *J. Power Sources*, 2012, **206**, 315.
13 S. Mukhopadhyay, T. Thompson, J. Sakamoto, A. Huq, J. Wolfenstine, J. L. Allen, N. Bernstein, D. A. Stewart and M. D. Johannes, *Chem. Mater.*, 2015, **27**, 3658.
14 T. Thompson, A. Sharafi, M. D. Johannes, A. Huq, J. L. Allen, J. Wolfenstine and J. Sakamoto, *Adv. Energy Mater.*, 2015, **5**, 1500096.
15 N. Janani, S. Ramakumar, S. Kannan and R. Murugan, *J. Am. Ceram. Soc.*, 2015, **98**, 2039.
16 K. Ishiguro, H. Nemori, S. Sunahiro, Y. Nakata, R. Sudo, M. Matsui, Y. Takeda, O. Yamamoto and N. Imanishi, *J. Electrochem. Soc.*, 2014, **161**, A668.
17 G. Haxhillazi and H. Haeuseler, *J. Solid State Chem.*, 2004, **177**, 3045.
18 N. Vuletic, E. Prcić and C. Djordjevic, *Z. Anorg. Allg. Chem.*, 1979, **450**, 67.
19 L. Cheng, E. J. Crumlin, W. Chen, R. Qiao, H. Hou, A. Lux, V. Zorba, R. Russo, R. Kostecki, Z. Liu, K. Persson, W. Yang, J. Cabana, T. Richardson, G. Chen and M. Doeff, *Phys. Chem. Chem. Phys.*, 2014, **16**, 18294.
20 W. G. Zeier, S. Zhou, B. Lopez-Bermudez, K. Page and B. C. Melot, *ACS Appl. Mater. Interfaces*, 2014, **6**, 10900.
21 V. Thangadurai and W. Weppner, *Adv. Funct. Mater.*, 2005, **15**, 107.
22 V. Thangadurai, S. Narayanan and D. Pinzaru, *Chem. Soc. Rev.*, 2014, **43**, 4714.
23 E. Hanc, W. Zając and J. Molenda, *Solid State Ionics*, 2014, **262**, 617.
24 S. Ohta, J. Seki, Y. Yagi, Y. Kihira, T. Tani and T. Asaoka, *J. Power Sources*, 2014, **265**, 40.
25 S. Song, D. Sheptyakov, A. M. Korsunsky, H. M. Duong and L. Lu, *Mater. Des.*, 2016, **93**, 232.
26 R. D. Shannon, *Acta Crystallogr., Sect. A: Cryst. Phys., Diffr., Theor. Gen. Cryst.*, 1976, **32**, 751.